Acoustic emission study of the TDCB test of microcapsules filled self-healing polymer

Gábor SZEBÉNYI[1,2*], Tibor CZIGÁNY[1,2], Brúnó VERMES[1], Xiao Ji YE[3,4], Min Zhi RONG[3], Ming Qiu ZHANG[3]

[1] Department of Polymer Engineering, Faculty of Mechanical Engineering, Budapest University of Technology and Economics, Műegyetem rkp. 3., H-1111 Budapest, Hungary

[2] MTA–BME Research Group for Composite Science and Technology, Műegyetem rkp. 3., H-1111 Budapest, Hungary

[3] Key Laboratory for Polymeric Composite and Functional Materials of Ministry of Education, GD HPPC Lab, School of Chemistry and Chemical Engineering, Sun Yat-Sen University, 510275 Guangzhou, P. R. China

[4] Guangdong Provincial Public Laboratory of Analysis and Testing Technology, China National Analytical Center, 510070 Guangzhou, P. R. China

* corresponding author: szebenyi@pt.bme.hu, +36-1-463-1466

E-mail addresses:

Gábor SZEBÉNYI – szebenyi@pt.bme.hu

Tibor CZIGÁNY- czigany@pt.bme.hu

Brúnó VERMES - vermesbruno@gmail.com

Xiao Ji YE - 562054764@qq.com

Min Zhi RONG - cesrmz@mail.sysu.edu.cn

Ming Qiu ZHANG - ceszmq@mail.sysu.edu.cn

Abstract

The failure process of self-healing microcapsule filled epoxy composites was investigated with Acoustic Emission (AE) measurement during tapered double cantilever beam (TDCB) tests. Unfilled, epoxy microcapsule filled and self-healing microcapsule (dual-microcapsules consisting of epoxy capsules and trifluoromethanesulfonic acid (TfOH) capsules) filled epoxy matrix specimens were compared. It was found that with acoustic emission measurements reliable data can be retrieved about the nature and progress of crack propagation and failure. Comparing the unfilled and the microcapsule filled specimens, considerably more AE hits were detected in the latter cases due to the cracks of capsules and capsule-matrix debonding, which was confirmed by scanning electron microscopy investigations. Also, key differences were observed in the shape of the sum of AE hits curves and amplitude ranges of detected AE hits. Uniform distribution of the healing agent was demonstrated by energy-dispersive X-ray spectroscopy.

Keywords

self-healing, acoustic emission, fracture analysis, microcapsules

1. Introduction

Multi-functional, self-healing materials are nowadays an important topic in material science as more and more polymer and polymer composite parts are used in safety-critical applications. Self-healing polymers can provide increased service time and reliability by the repair of the emerging micro-cracks during operation [1-3]. While the development of self-healing polymer resin systems is in progress, the failure methods of the complex self-healing systems have to be also thoroughly investigated.

Many researchers use the concept of solid polymer shells filled with liquid healing agent, dispersed in polymer matrix, in order to achieve the desired repairing capability [4]. Functionally, as the propagating microcrack reaches and cracks open the solid shell, the released low-viscosity healing agent fills the crack due to capillary action and polymerizes on contact with the catalyst. Despite their similar approach, distinct methods reported a variety of quality and preparation processes of self-healing polymers since the breakthrough made by White and co-workers [5]. One of the most extensively used healing agent is dicyclopentadiene (DCPD) [5-10] contained in urea-formaldehyde (UF) copolymer shells. It works through ring-opening metathesis polymerization (ROMP) and requires solid (Grubbs' first generation) catalyst to be dispersed in the applied epoxy matrix. Others use different materials for the shells [11], or stick the catalyst to its wall instead of dispersing in the matrix [12]. Another widely used healing agent is epoxy resin [13-16], which needs a hardener component to react with so as to establish cross links, hence curing the crack. Considering the processing and the application circumstances, each method may require further parameter optimization by using alternative catalysts [17], smaller capsule sizes [18], etc. It is, however, always necessary to analyze the mechanical and other properties of the ready composite and set the results against the reference samples to conclude the

microcapsules' and the healing agents' effects to the material. The rupture of tapered double cantilever beam (TDCB) samples and acoustic emission (AE) monitoring [19] provide information about the proceeding failure, whilst scanning electron microscope (SEM) analysis visualizes the result on the surface of the crack [20]. With energy-dispersive X-ray spectroscopy (EDS), the elemental map of a fracture surface can be prepared, making the visualization of the self-healing compound possible [21, 22].

The objective of the present work is to apply the AE technique to analyze the above-mentioned self-healing composites fracture behavior during TDCB testing to acquire further information on the mechanism and efficiency of the capsules' cracking and healing capability for future optimization.

2. Material and methods

2.1. Materials

High performance cycloaliphatic epoxy resin (trade name: Araldite® CY 179), supplied by Huntsman Advanced Materials, was used as the matrix. Methyl hexahydrophthalic anhydride (MHHPA) purchased from Energy Chemical, Shanghai, China, acted as its hardener. Hycat™ AO-4, produced by Dimension Technology Chemical Systems, Inc., was employed as the catalyst. Diglycidyl ether of bisphenol A (trade name: EPON 828), supplied by Shell Co., served as the polymerizable component of the healing agent. TfOH was obtained from Sigma–Aldrich and acts as the hardener component of the healing agent.

Preparation of the healing capsules, including epoxy microcapsules (~130 μm) and TfOH microcapsules (~6 μm), and self-healing epoxy composites has been described elsewhere [23].

The TDCB specimens with groove length of 55 mm were made following Brown et al. [24] For the convenience of discussion, three types of TDCB specimens were fabricated and characterized. They are: unfilled epoxy ("A" type), epoxy filled with 10 wt% epoxy-loaded capsules ("B" type), and epoxy filled with 10 wt% epoxy capsules and 0.6 wt% TfOH capsules ("C" type).

2.2. Experimental

The TDCB tests were carried out using a Zwick Z250 (Zwick, Ulm, Germany) computer controlled tensile tester equipped with a 20 kN capacity load cell. The test speed was 0.3 mm min^{-1}. The specimens were pre-notched by a sharp razor blade to facilitate defined crack formation. The crack propagation was monitored by a digital camera during the tests (Fig 1).

The Acoustic Emission (AE) signals emerging during the failure of the specimens were recorded by a Sensophone AEPC-40/4 (Gereb & Co., Budapest, Hungary) type device equipped with a Physical Acoustic Corporation Micro30S (Physical Acoustic Corporation, Princeton, USA) microphone. The microphone was fixed to the surface of the specimen by a plastic clip. The contact surface of the microphone and the specimen was covered with

silicon grease. The recorder frequency range was 100 – 600 kHz, and the applied threshold was set to 20 dB. Logarithmic amplifying was applied.

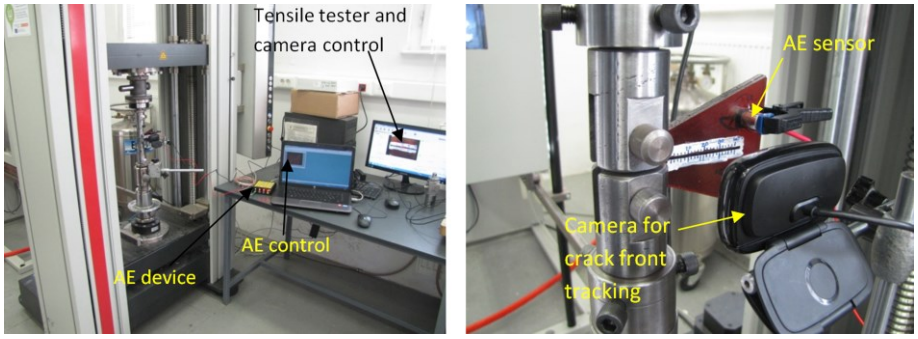

Fig 1 Test setup of the TDCB test (left) and positioning of the AE sensor and the crack tracking camera (right)

Scanning Electron Microscopy (SEM) investigations were carried out on the fracture surfaces of the broken specimens by a JEOL JSM-6380LA (Jeol Ltd., Akishima, Japan) microscope. The sample surfaces were gold sputter coated to achieve electrical conductivity.

Energy-dispersive X-ray spectroscopy (EDS) investigations were carried out on the fracture surface of a broken self-healed specimen (C Healed) using a Zeiss SEM (Carl Zeiss AG, Oberkochen, Germany) equipped by an EDAX EDS device with an Octane Silicon Drift Detector (EDAX Inc., Mahwah, USA). The sample was gold spur coated to achieve surface electrical conductivity.

3. Results and discussion

During the TDCB tests, samples A and B were loaded by constant crosshead displacement up to complete fracture (50 mm crack front position, Fig 2). Sample C was loaded up to the first crack jump, after which the crosshead reversed to close the crack, 5 minutes curing time was provided for the healing process and, finally, in a second constant crosshead displacement loading, the specimen was tested to complete fracture.

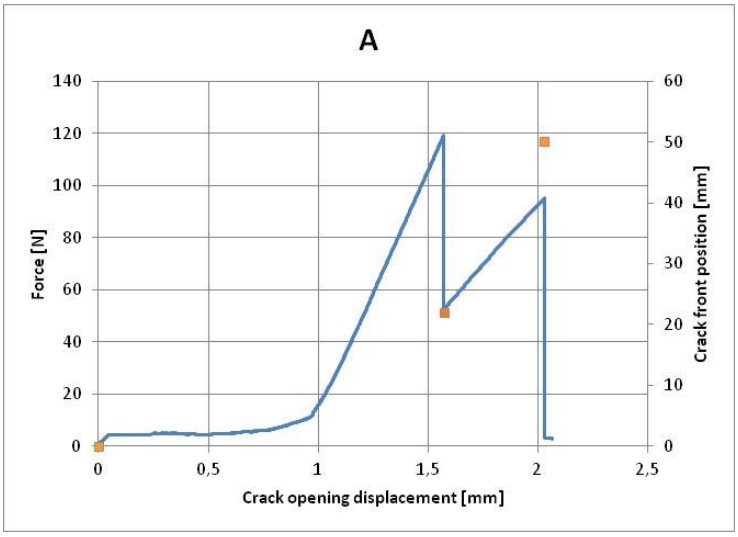

Fig 2 Recorded force and crack front position curves of an unfilled (A) specimen as a function of crack opening displacement

The tests showed good results. The crack tracking was accurate, also the AE measurements provided a sufficient number of hits. The position of the sum of all hits jumps corresponded to the actual crack jumps present in the force – crack opening displacement curves recorded by the tensile tester and the visual crack front propagation observations (Fig 3).

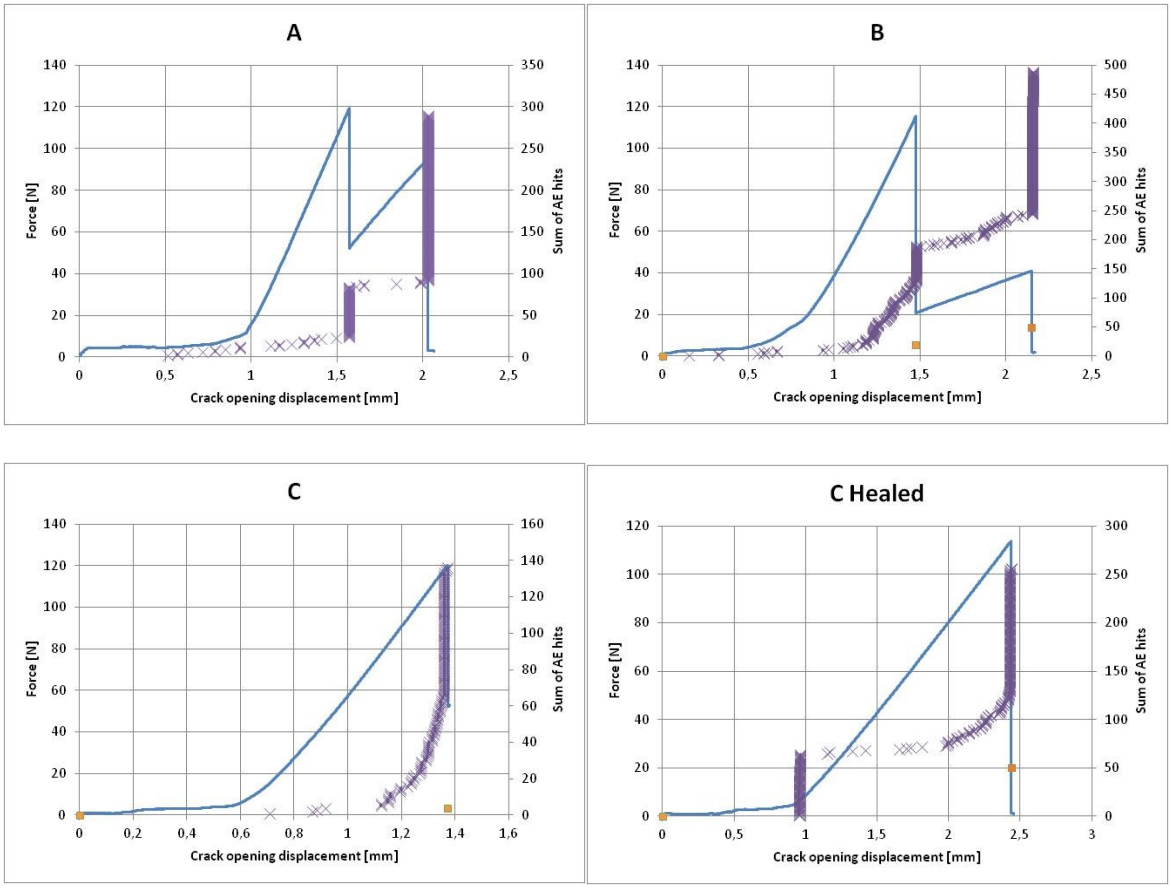

Fig 3 Recorded force and sum of AE hits curves of an unfilled (A), epoxy microcapsule filled (B), and a self-healing specimen before (C) and after healing (C Healed) as a function of crack opening displacement

Many more hits were recorded in case of the microcapsule filled samples (A – 289, B - 488, C – 136, C Healed – 256, C+C Healed - 392). Also, the shapes of the sum of hits curves are quite different: significantly more hits were recorded in the case of the microcapsule filled samples (B, C) before the first crack jump. This can indicate the cracking of the microcapsules and damages at the microcapsule-resin interface. Also, there is a significant

difference in the progress of the curve: in the case of the neat resin sample (A) the sum of all hits curve shows a prompt jump at the crack jump (Fig 3 – A), while in the case of the microcapsule filled samples (Fig 3 – B and C) the jump is not so steep, but is foreshadowed by a constant, steady increase in the sum of all hits curve.

In the case of the healed sample, the start of the cracking of the specimen at the healed surface can be clearly observed at around 1 mm crack opening displacement; at the second peak, the run of the sum of all hits curve is similar to the first recorded curve of the same specimen. It can also be observed that the high amplitude hit for the first crack jump is missing, only the middle range amplitude hits are present.

The analysis of the AE amplitudes shows that the crack jump can be identified by the high amplitude hits above 100 dB. For better comparison, we have prepared the histograms of the AE amplitudes and the AE energies of the samples (Fig 4-5). To be able to compare the self-healing samples to the reference samples (A and B), we had to add the two test sections of the self-healing sample (the total hits of the C and C Healed tests), because this represents the cracking of the whole sample. In the comparison of the microcapsule filled (B and C+C Healed) samples to the neat resin sample, clear differences can be seen. In the case of the AE amplitudes, the unfilled microcapsule containing samples provided significantly more high amplitude hits (above the 50 dB region), the self healing agent filled microcapsule containing samples provided much more low amplitude hits (below 30 dB). The difference between the unfilled and filled microcapsule containing samples can be explained by their different acoustic behaviour, the self-healing agent filled into the microcapsules can have a damping effect.

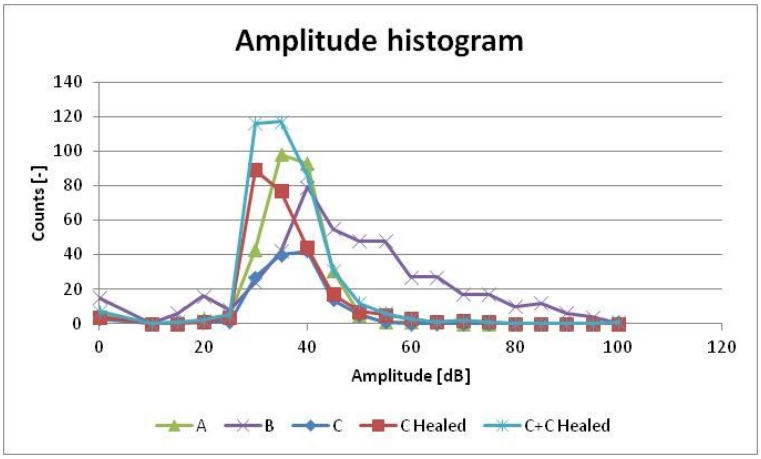

Fig 4 AE Amplitude histograms of the tested samples

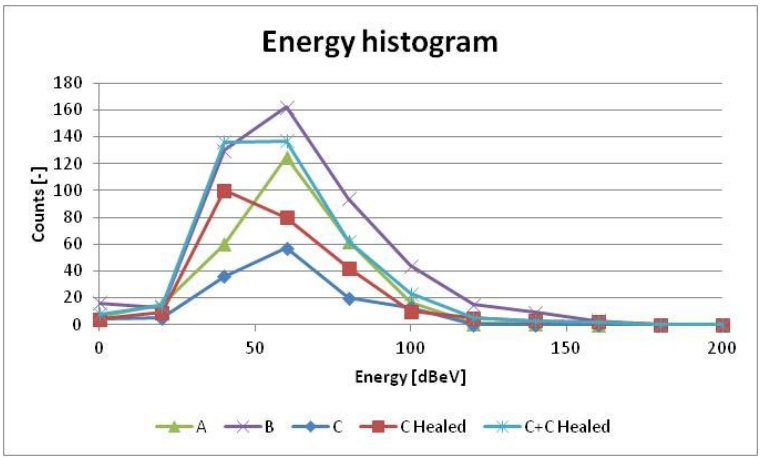

Fig 5 AE energy histograms of the tested samples

To investigate their fracture behavior SEM, micrographs have been prepared from the fracture surfaces of the broken specimens (A, B and C Healed). Some characteristic micrographs are presented in Fig 6-8. The micrographs confirm the presence of the microcapsules in samples B and C. In some regions, debonding along the interface between the microcapsules and the matrix can be observed. Some microcapsules are fractured.

Instead of the clear splitting of the capsules, only holes in some capsule shells are present. This can indicate weak adhesion between the matrix and the microcapsules, so most of the differences in the AE data are caused by the debonding.

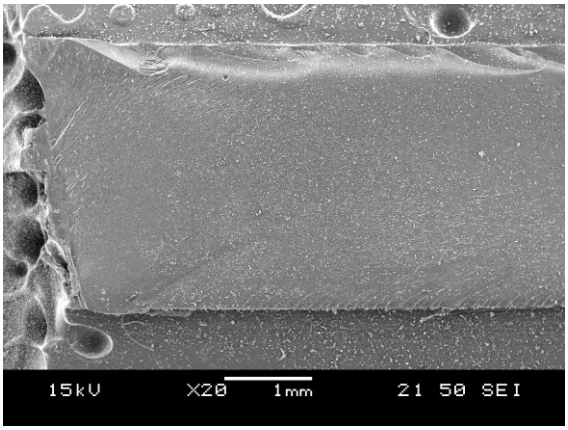

Fig 6 SEM micrograph of sample “A”

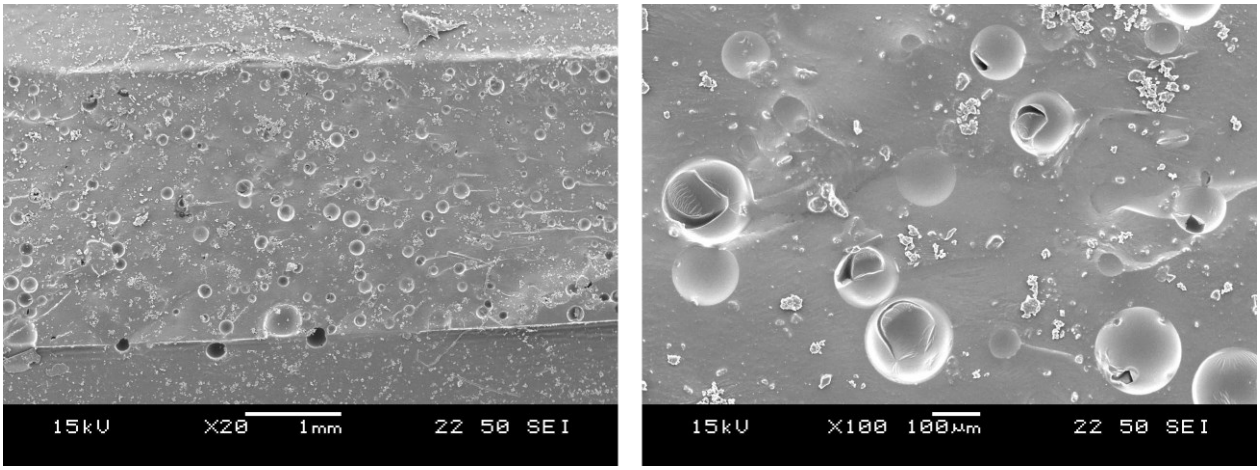

Fig 7 SEM micrographs of sample “B”

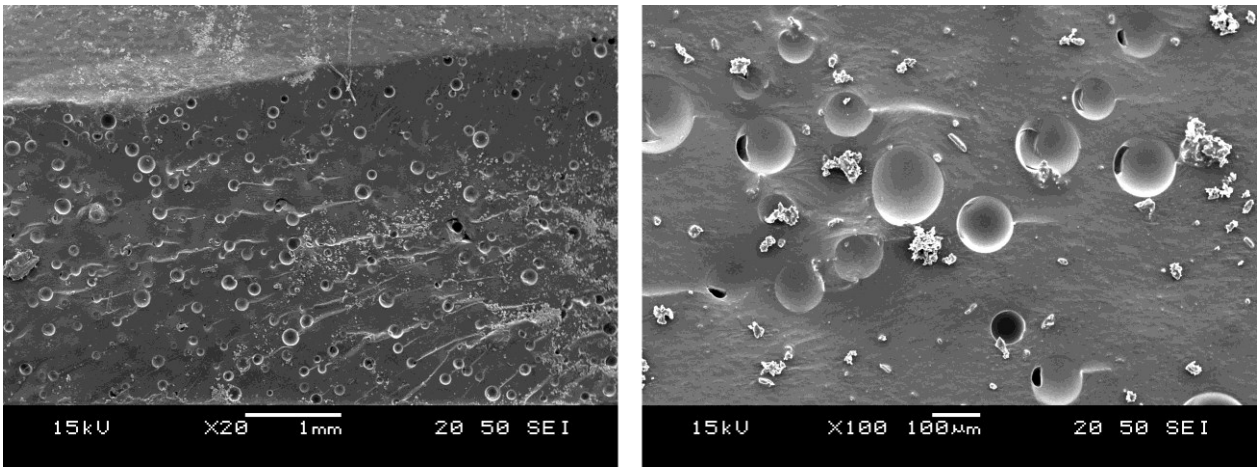

Fig 8 SEM micrographs of sample “C Healed”

Energy-dispersive X-ray spectroscopy (EDS) investigations were carried out on the fracture surface of a broken self-healed specimen (C Healed) to check if the sulphur containing self-healing agent has reached the crack. The map of the detected sulfur (which originated from TfOH) is presented in Fig 9. In the map, sulfur is almost uniformly present in the whole fracture surface, except some locations, mostly at the microcapsule surfaces. Clearly, the healing agent has been released from the broken microcapsules and covered the crack surface as expected.

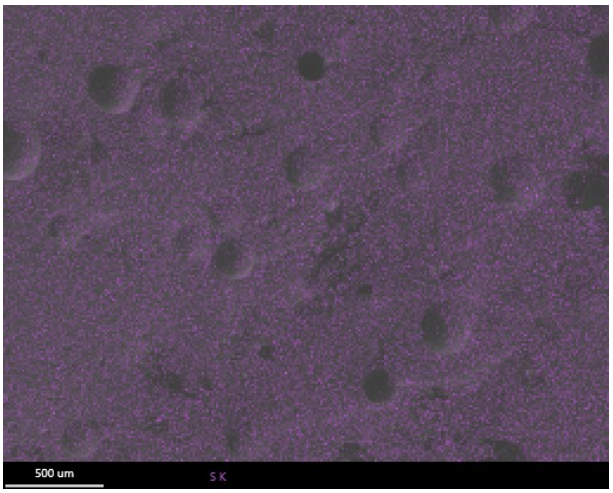

Fig 9 SEM micrograph of sample “C Healed” with the detected sulphur location EDS overlay (purple dots)

4. Conclusions

While the wanted self-healing property develops, microcapsules cause significant change in the material's integrity, and hence in its mechanical properties. In the case of microencapsulated self-healing polymer composites, the fracture of the microcapsules during the failure process is one of the key requirements among others - such as the quality and the quantity components taking part in the chemical reaction, the healing performance is therefore controlled not only by chemical, but mechanical properties as well.

With acoustic emission, reliable data were collected by detecting the numbers of hits in function of displacement and crack propagation, which correlates with the progress of failure. The sum of these hits were significantly higher in case of the encapsulated material, which can indicate cracking of the capsules and the capsule-matrix interface.

Further information can be retrieved from the AE amplitudes in each case as crack jumps can be identified by higher amplitude hits, for instance.

Adhesion between capsules and matrix should have sufficient strength to prevent the separation of the interface to give a full play to self-healing. Self-healing behaviour was observed in specimens, although SEM images have shown both fractured and separated microcapsules. This means that, after strengthening the adhesion, the same performance would be achievable even with lower capsule ratio.

Uniform distribution of the healing agent, essential to create uniformly healed material, was observed on the crack surface by using energy-dispersive X-ray spectroscopy.

Acknowledgements

This work is connected to the scientific program of the 'Development of quality-oriented and harmonized R+D+I strategy and functional model at BME' project. This project is supported by the New Széchenyi Plan (Project ID:TÁMOP-4.2.1/B-09/1/KMR-2010-0002) and the Sino-Hungarian Scientific and Technological Cooperation Project (Grant: TÉT_12_CN-1-2012-0010). This paper was supported by National Research, Development and Innovation Office - NKFIH, OTKA K 116070. Gábor Szebényi acknowledges the financial support received through János Bolyai Scholarship of the Hungarian Academy of Sciences. M. Q. Zhang thanks the support of the Natural Science Foundation of China (Grant: 51333008).

References

[1] M.Q Zhang, M.Z Rong. Self-healing Polymers and Polymer composites, Wiley. 2011

[2] X.J Ye, Y. Zhu, Y.C Yuan, Y.X Song, G.C Yang, M.Z Rong, M.Q Zhang. Fatigue life extension of epoxy materials using ultrafast epoxy-SbF5 healing system introduced by manual infiltration. Express Polym Lett 2015;9(3):177.

[3] M.Q Zhang, Polymer self-heals in seconds, Express Polym Lett 2015;9(2):84.

[4] D.Y Zhu, M.Z Rong, M.Q Zhang. Self-healing polymeric materials based on microencapsulated healing agents: From design to preparation. Prog Polym Sci 2015;49:175.

[5] S.R White, N.R Sottos, P.H Guebelle, J.S Moore, M.R Kessler, S.R Sriram, E.N Brown, S. Viswanathan. Autonomic healing of polymer composites. Nature 2001;409:794.

[6] M.R Kessler, N.R Sottos, S.R White. Self-healing structural composite materials. Compos Part A-Appl S 2003;34:743.

[7] S.R White, N.R Sottos, P.H Geubelle, J.S Moore, S.R Sriram, M.R Kessler, E.N Brown. Multifunctional automatically healing composite material. 6518330 B2, USA, 2003.

[8] B.J Blaiszik, N.R Sottos, S.R White. Nanocapsules for self-healing materials. Compos Sci Technol 2008;68(3):978.

[9] E.N Brown, M.R Kessler, N.R Sottos, S.R White. In situ poly(urea-formaldehide) microencapsulation of dicyclopentadiene. J Microencapsul 2003;20(6):719.

[10] G.O Wilson, M.M Caruso, N.T Reimer, S.R White, N.R Sottos, J.S Moore. Evaluation of Ruthenium Catalysts for Ring-Opening Metathesis Polymerization-Based Self-Healing Applications. Chem Mater 2008:20(10):3288.

[11] H. Zhang, P. Wang, J. Yang. Self-healing epoxy via epoxy–amine chemistry in dual hollow glass bubbles. Compos Sci Technol 2014:94(9):23.

[12] A.F Skipor, S.M Scheifer, B. Olson. Self-healing polymer compositions. US 2004/0007784 A1, USA, 2004.

[13] T. Yin, M.Z Rong, M.Q Zhang, G.C Yang. Self-healing epoxy composites – Preparation and effect of the healant consisting of microencapsulated epoxy and latent curing agent. Compos Sci Technol 2007;67(2):201.

[14] Y.C Yuan, M.Z Rong, M.Q Zhang. Preparation and characterisation of microencapsulated polythiol. Polymer 2008;49(10):2531.

[15] A. Czeller, T. Czigány In: `ECCM15 – 15th European Conference on Composite Materials, Venice, 2012. paper 1353.

[16] H. Jin, C.L Mangun, D.L Stradley, J.S Moore, N.R Sottos, S.R White. Self-healing thermoset using encapsulated epoxy-amine healing chemistry. Polymer 2012;53(2):581.

[17] J.D Rule, E.N Brown, N.R Sottos, S.R White, J.S Moore. Wax-Protected Catalyst Microspheres for Efficient Self-Healing Materials. Adv Mater 2005;17(2):205.

[18] J.D Rule, N.R Sottos, S.R White. Effect of microcapsule size on the performance of self-healing polymers. Polymer 2007;48:3520.

[19] I.Z Halasz, G. Romhany, A. Kmetty, T. Barany, T. Czigany. Failure of compression molded all-polyolefin composites studied by acoustic emission. Express Polym Lett 2015;9(3):321.

[20] T.S.B Naser, K. Bobor, Gy. Krállics. Tensile behavior of multiple forged 6082 Al alloy. Period Polytech Mech Eng 2014;58(2):113.

[21] N.Y Ning, Z.P Zheng, L.Q Zhang, M. Tian. An excellent ozone-resistant polymethylvinylsiloxane coating on natural rubber by thiol-ene click chemistry. Express Polym Lett 2015;9(6):490.

[22] H.Y Gu, Z.Y Qi, W. Wu, Y. Zeng, L.X Song. Superhydrophobic polyimide films with high thermal endurance via UV photo-oxidation. Express Polym Lett 2014;8(8):588.

[23] X.J Ye, Y.X Song, Y. Zhu, G.C Yang, M.Z Rong, M.Q Zhang. Self-healing epoxy with ultrafast and heat-resistant healing system processable at elevated temperature. Compos Sci Technol 2014;104:40.

[24] E.N Brown, N.R Sottos, S.R White. Fracture testing of a self-healing polymer composite. Exp Mech 2002;42(4):372.

Figure captions:

Fig 1 Test setup of the TDCB test (left) and positioning of the AE sensor and the crack tracking camera (right)

Fig 2 Recorded force and crack front position curves of an unfilled (A) specimen as a function of crack opening displacement

Fig 3 Recorded force and sum of AE hits curves of an unfilled (A), epoxy microcapsule filled (B), and a self-healing specimen before (C) and after healing (C Healed) as a function of crack opening displacement

Fig 4 AE Amplitude histograms of the tested samples

Fig 5 AE energy histograms of the tested samples

Fig 6 SEM micrograph of sample “A”

Fig 7 SEM micrographs of sample “B”

Fig 8 SEM micrographs of sample “C Healed”

Fig 9 SEM micrograph of sample “C Healed” with the detected sulphur location EDS overlay (purple dots)